

Supporting Information

A New Strategy to Effectively Alleviate Volume Expansion and Enhance Conductivity of Hierarchical MnO@C Nanocomposites for Lithium Ion Batteries

Zhe Cui,^{a,b} Qian Liu,^c Chaoting Xu,^a Rujia Zou^{a,*}, Jianhua Zhang,^a Wenlong Zhang,^a
Guoqiang Guan,^a Junqing Hu^{a,*} and Yangang Sun^{b,*}

^a State Key Laboratory for Modification of Chemical Fibers and Polymer Materials,
College of Materials Science and Engineering, Donghua University, Shanghai 201620,
China

^b College of Chemistry and Chemical Engineering, Shanghai University of
Engineering Science, Shanghai 201620, China

^c Department of Physics, Donghua University, Shanghai 201620, China

*Corresponding author, E-mail: rjzou@dhu.edu.cn

hu.junqing@dhu.edu.cn

syg021@sues.edu.cn

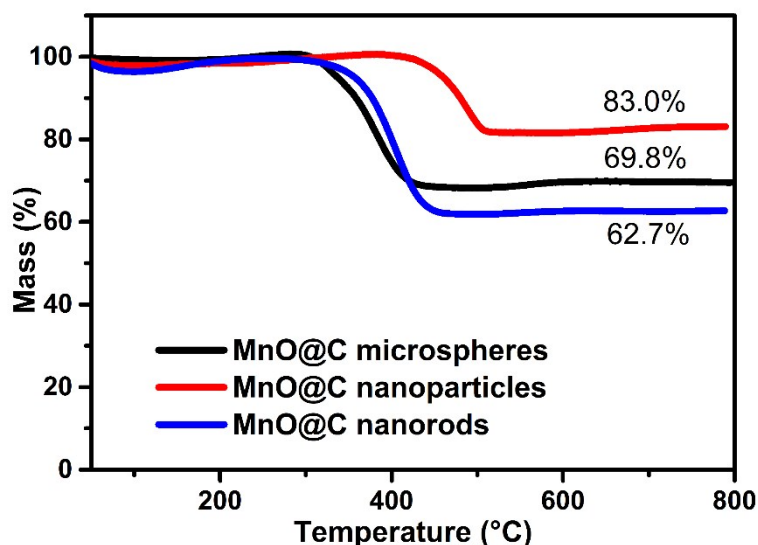


Fig. S1 TG curves of MnO@C microspheres, MnO@C nanoparticles and MnO@C nanorods. In order to ascertain carbon content for MnO@C hierarchical microspheres, MnO@C nanorods and MnO@C nanoparticles, the TGA measurement has been conducted. As can be seen from Fig. 2, for MnO@C microspheres, the weight loss of $\sim 0.86\%$ below $200\text{ }^{\circ}\text{C}$ should be ascribed to the adsorption of water,¹ and the weight gain of $\sim 1.8\%$ between $200\sim 350\text{ }^{\circ}\text{C}$ is due to the slightly oxidation of MnO to Mn_2O_3 .² Subsequently, the huge weight loss of 32.44% is mainly attributed to the combustion of carbon to CO_2 and partial oxidation of MnO into Mn_2O_3 .² Finally, it can be observed that after $500\text{ }^{\circ}\text{C}$, the weight gains of $\sim 1.5\%$ and remains no change until $800\text{ }^{\circ}\text{C}$, indicating the entirely oxidation of MnO to Mn_2O_3 .³ According to previous reports,^{4,5,6} MnO transforms to Mn_2O_3 after heating to $1050\text{ }^{\circ}\text{C}$ in an oxygen atmosphere. Therefore, it is believable that the final weight of $\sim 69.8\%$ is entirely corresponding to Mn_2O_3 transformed from MnO, which suggests that the original MnO is calculated to $\sim 62.7\%$, and the carbon content should be $\sim 37.3\%$. The carbon content is approximately comparable to that of other MnO/C composition derived from Mn-MOF.^{1,7,8} Similarly, the carbon content of MnO@C nanoparticles and MnO@C nanorods is calculated to $\sim 26.4\%$ and $\sim 43.7\%$, respectively.

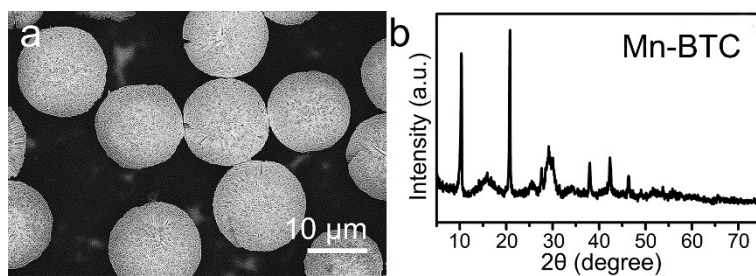


Fig. S2 a) The low magnification SEM image. b) XRD pattern of Mn-BTC.

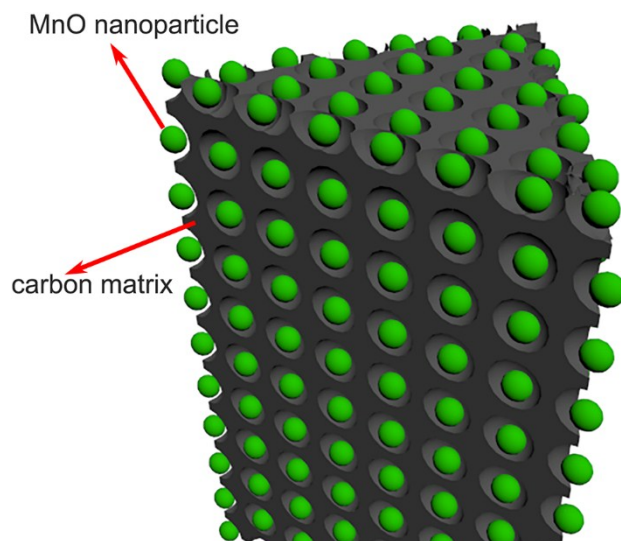


Fig. S3 The schematic drawing for inner structure of single nanorod in MnO@C microsphere.

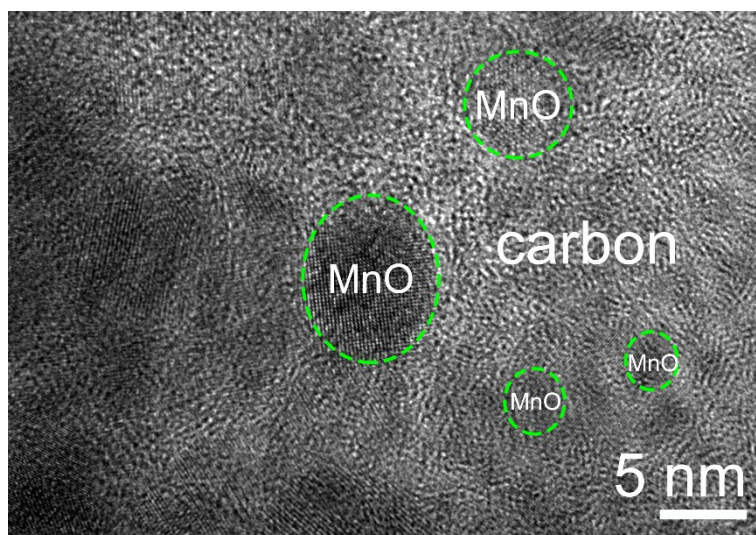


Fig. S4 The HRTEM image of MnO@C microsphere taken from the middle area of single nanorod.

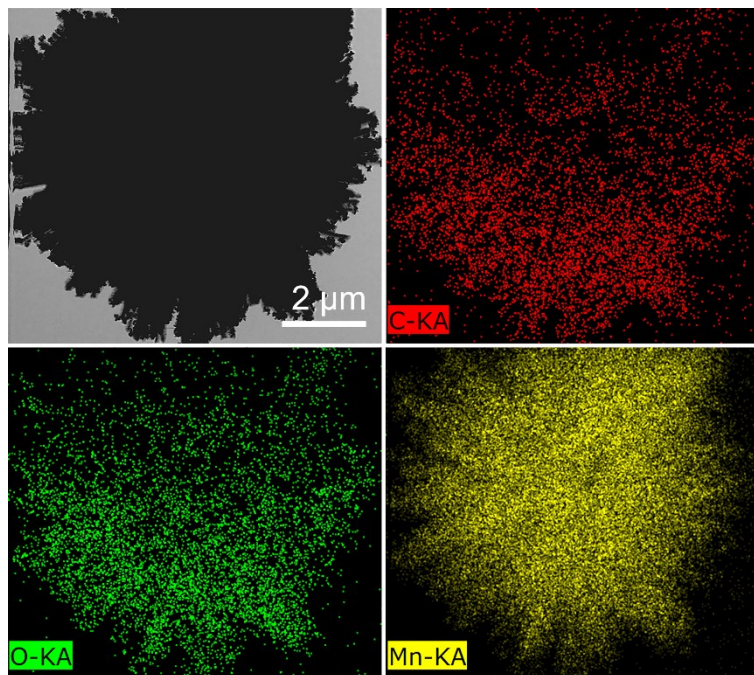


Fig. S5 EDS mapping images of as-prepared MnO@C microsphere.

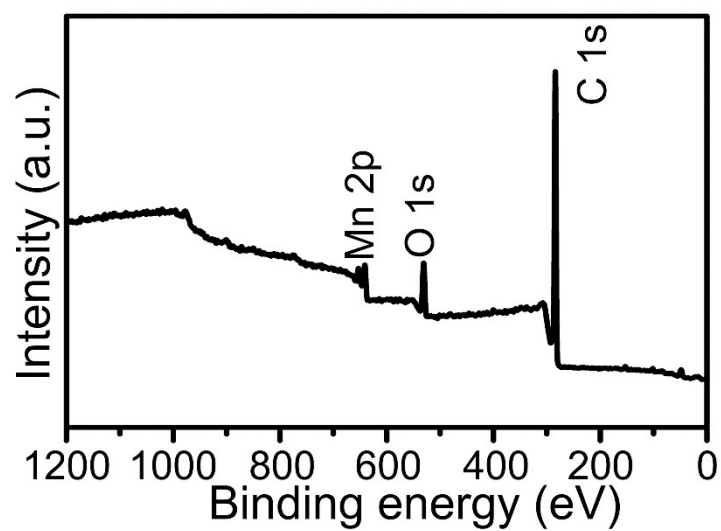


Fig. S6 XPS survey spectrum of MnO@C microspheres.

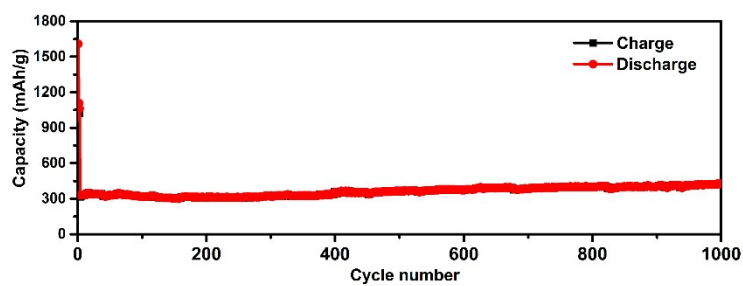


Fig. S7 Cycling performance of MnO@C microsphere tested at 10 C for 1000 cycles.

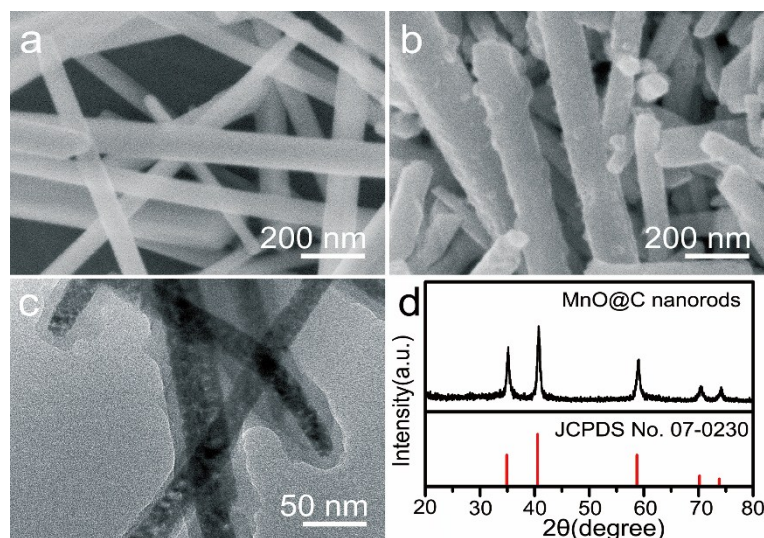


Fig. S8 a) SEM images of MnCO_3 nanorods. b-d) SEM image (b), TEM image (c) and XRD patterns (d) of MnO@C nanorods. The MnCO_3 nanorods (Figure S5a) in a diameter of 70~140 nm were firstly synthesized through a hydrothermal route. The final product MnO@C nanorod has a diameter of 150~200 nm (Figure S5b) and an apparent carbon layer is in a thickness of 10~20 nm (Figure S5c). The XRD patterns (Figure S5d) can be also well-indexed to cubic MnO (JCPDS No. 07-0230).

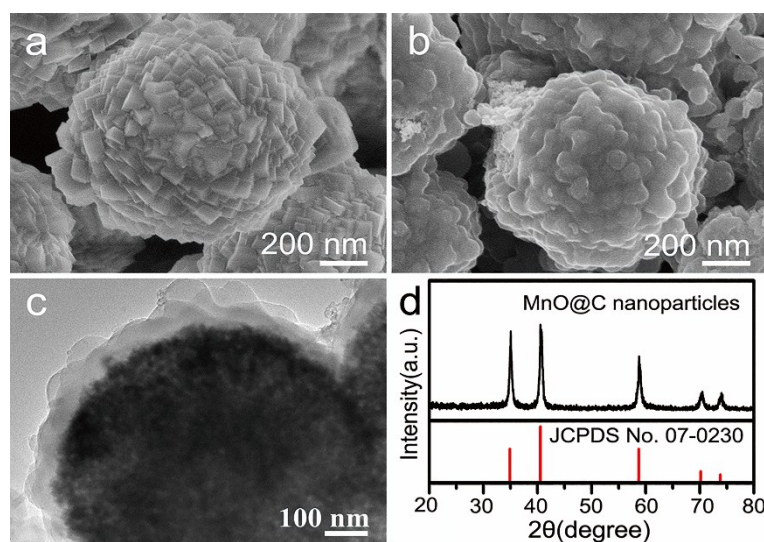


Fig. S9 a) SEM images of MnCO_3 nanoparticles. b-d) SEM image (b), TEM image (c) and XRD patterns (d) of MnO@C nanoparticles. The MnCO_3 microsphere aggregated by nanoparticles was first prepared as show in Fig S6a. After coated by PDA and carbonized in an inert atmosphere, the MnO@C nanoparticles was obtained (Figure S6b). From the TEM image (Figure S6c), the carbon layer with a thickness of ~50 nm

could be obviously observed and the XRD pattern in Figure S6d further confirmed its structure information which could be indexed into the cubic MnO (JCPDS No. 07-0230).

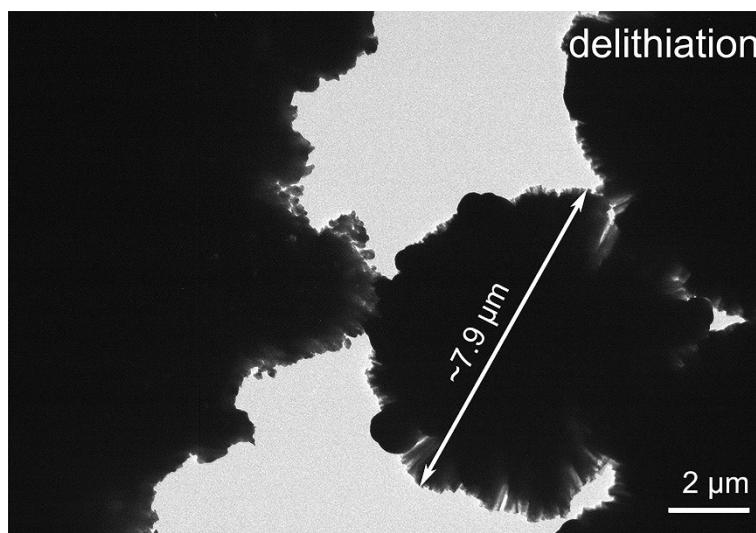


Fig. S10 The TEM image of MnO@C hierarchical microsphere after lithiation.

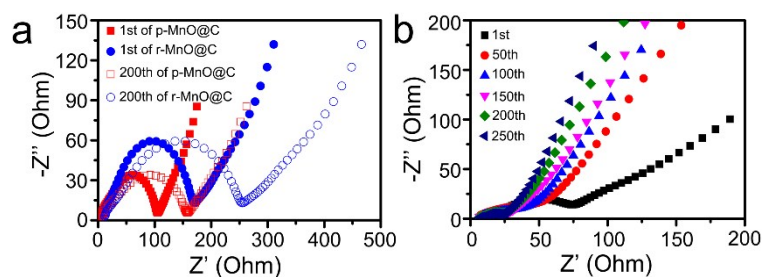


Fig. S11 a) Nyquist plots of MnO@C nanorods and MnO@C nanoparticles. b) Nyquist plots of MnO@C microspheres in different cycles.

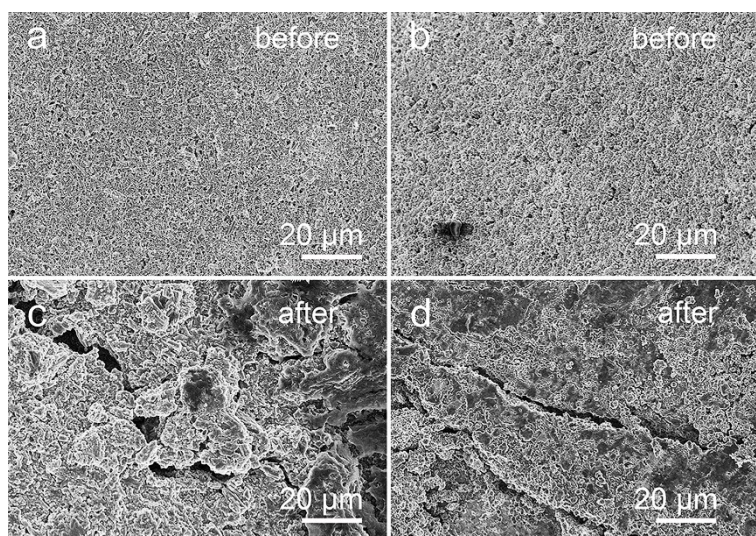


Fig. S12 SEM images of the electrodes before cycles for MnO@C nanorods (a) and MnO@C nanoparticles (b), and after cycles for MnO@C nanorods (c) and MnO@C nanoparticles (d).

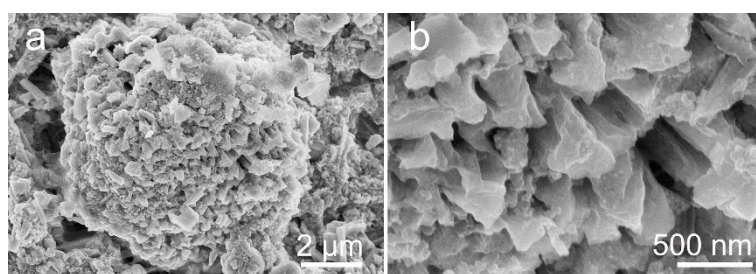


Fig. S13 a) The low magnification and b) high magnification SEM images of MnO@C microspheres in the electrode after cycles.

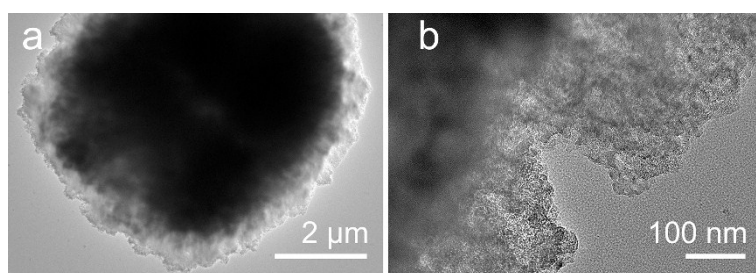


Fig. S14 TEM images of MnO@C microsphere after 1000 cycles.

Reference:

- 1 F. C. Zheng, G. L. Xia, Y. Yang and Q. W. Chen, *Nanoscale*, 2015, **7**, 9637-9645.
- 2 C. X. Yang, Q. M. Gao, W. Q. Tian, Y. L. Tan, T. Zhang, K. Yang and L. H. Zhu, *J. Mater. Chem. A*, 2014, **2**, 19975-19982.
- 3 X. J. Jiang, W. Yu, H. Wang, H. Y. Xu, X. Z. Liu and Y. Ding, *J. Mater. Chem. A*,

2016, **4**, 920-925.

4 M. I. Zaki, M. A. Hasan, L. Pasupulety and K. Kumari, *Thermochim. Acta*, 1997, **303**, 171-181.

5 Y. Xia, Z. Xiao, X. Dou, H. Huang, X. H. Lu, R. J. Yan, Y. P. Gan, W. J. Zhu, J. P. Tu, W. K. Zhang and X. Y. Tao, *ACS Nano*, 2013, **7**, 7083-7092.

6 D. M. Kang, Q. L. Liu, R. Si, J. J. Gu, W. Zhang, D. Zhang, *Carbon*, 2016, **99**, 138-147.

7 F. C. Zheng, Z. C. Yin, H. Y. Xia, G. L. Bai and Y. G. Zhang, *Chem. Eng. J.*, 2017, **327**, 474-480.

8 D. Sun, Y. G. Tang, D. L. Ye, J. Yan, H. S. Zhou and H. Y. Wang, *ACS Appl. Mater. Interfaces*, 2017, **9**, 5254-5262.